研究成果の刊行に関する一覧表

書籍

該当なし

雑誌

発表者氏名	論文タイトル名	発表誌名	巻号	ページ	出版年
Arai, Y., Totoki, Y., Takahashi, H., Nakamura, H., Hama, N., Kohno, T., Tsuta, K., Yoshida, A., Asamura, H., Mutoh, M., Hosoda, F., Tsuda, H., Shibata, T.	Mouse model for ROS1-rearranged lung cancer.	PLoS One	8	e56010	2013
Ueno, T., Imaida, L., Yoshimoto, M., Hayakawa, T., Takahashi, M., Imai, T., Yanaka, A., Tsuta, K., Komiya, M., Wakabayashi, K., Mutoh, M.	Non-invasive X-ray micro-computed tomographic evaluation of indomethacin on urethane-induced lung carcinogenesis in mice.	Anticancer Res.	32	4773-4780	2012
Ueno, T., Teraoka, N., Takasu, S., Nakano, K., Takahashi, M., Yamamoto, M., Fujii, G., Komiya, M., Yanaka, A., Wakabayashi, K., Mutoh, M.	Suppressive effect of pioglitazone, a PPAR gamma ligand, on azoxymethane-induced colon aberrant crypt foci in KK-Ay mice.	Asian Pac. J. Cancer Prev.	13	4067-4073	2012
Ishino, K., Mutoh, M.,	Metabolic syndrome : A novel high-risk state for colorectal cancer.	Cancer Lett.			In press

Totsuka, Y., Nakagama, H.					
Shimura, M., Yamamoto, M., Fujii, G., Takahashi, M., Komiya, M., Noma, T., Tanuma, S., Yanaka, A., Mutoh, M.	Novel compound SK-1009 suppresses interleukin-6 expression through modulation of activation of nuclear factor-kappaB pathway.	Bio. Pharm. Bull.	35	2186-2191	2012
Takahashi, M., Mutoh, M., Ishigamori, R., Fujii, G., Imai, T.	Involvement of inflammatory factors in pancreatic carcinogenesis and preventive effects of anti-inflammatory agents.	Semin. Lmmunopathol.	35	203-227	2013
Hori, M., Onaya, H., Takahashi, M., Hiraoka, N., Mutoh, M., Kosuge, T., Nakagama, H.	Invasive ductal carcinoma developing in pancreas with severe Fatty infiltration.	Pancreas	41	1137-1139	2012
Yoshimoto, M., Hayakawa, T., Mutoh, M., Imai, T., Tsuda, K., Kimura, S., Umeda, IO., Fujii, H., Wakabayashi, K.	In vivo SPECT imaging with 111In-DOTA-c(RGDfK) to detect early pancreatic cancer in a hamster pancreatic carcinogenesis model.	J. Nucl. Med.	53	765-771	2012
Takasu, S., Mutoh, M.,	Lipoprotein lipase as a candidate target for cancer prevention/therapy.	Biochem. Res. Int.	2012	398697	2012

Takahashi, M., Nakagama, H.					
Matsubara, S., Takasu, S., Tsukamoto, T., Mutoh, M., Masuda, S., Sugimura, T., Wakabayashi, K., Totsuka, Y.	Induction of glandular stomach cancers in Helicobacter pylori-infected Mongolian gerbils by 1-nitrosoindole-3-acetonitrile.	Int. J. Cancer	130	259-266	2012
Ito, K., Ishigamori, R., Mutoh, M., Ohta, T., Imai, T., Takahashi, M.	A^y allele promotes azoxymethane-induced colorectal carcinogenesis via macrophage migration in hyperlipidemic/diabetic KK mice.	Cancer Sci.			In press
Komiya, M., Fujii, G., Takahashi, M., Iigo, M., Mutoh, M.	Prevention and intervention trials for colorectal cancer.	Jpn. J Clin. Oncol.			In press
○ Tanaka, T., Tanaka, T., Tanaka, M., Kuno, T.	Cancer chemoprevention by citrus pulp and juices containing high amounts of beta-cryptoxanthin and hesperidin.	J. Biomed. Biotechnol.	Volume 2012	Article ID 516981	2012
○Tanaka, T.	Development of an inflammation-associated colorectal cancer model and its application for research on carcinogenesis and chemoprevention.	Int. J. Inflammation	Volume 2012	Article ID 658786	2012
○ Tanaka, T., Shimizu, M., Moriwaki, H.	Cancer chemoprevention by carotenoids.	Molecules	17	3202-3242	2012
Kuno, T., Tsukamoto, T., Hara, A,, ○ Tanaka, T.	Cancer chemoprevention through the induction of apoptosis by natural compounds.	J. Biophys. Chem.	3	156-173	2012
Mann, P.C., Vahle, J.,	International harmonization of toxicologic pathology nomenclature: an overview and review of basic	Toxicol. Pathol.	40	7S-13S	2012

Keenan, C.M., Baker, J.F., Bradley, A.E., Goodman, D.G., Harada, T., Herbert, R., Kaufmann, W., Kellner, R., Nolte, T., Rittinghausen, S., ○Tanaka T.	principles.				
○Tanaka, T.	Animal models of carcinogenesis in inflamed colorectum: Potential use in chemoprevention study.	Curr. Drug Targets	13	1689-1697	2012
Katsurano, M., Niwa, T., Yasui, Y., Shigematsu, Y., Yamashita, S., Takeshima, H., Lee, M.S., Kim, Y.J., ○Tanaka, T., Ushijima, T.	Early-stage formation of an epigenetic field defect in a mouse colitis model, and non-essential roles of T- and B-cells in DNA methylation induction.	Oncogene	31	342-351	2012
Hata, K., Kubota, M., Shmizu, M., Moriwaki, H., Kuno, T., ○Tanaka, T., Hara, A., Hirose, H.	Monosodium glutamate-induced diabetic mice are susceptible to azoxymethane-induced colon tumorigenesis.	Carcinogenesis	33	702-707	2012
Shimasaki, T., Ishigaki, Y., Nakamura, Y., Takata, T., Nakaya, N., Nakajima, H., Satoh, I., Zhao, X., Kitano, A., Kawakami, K., ○Tanaka, T., Takegami, T., Tomosugi, N., Minamoto, T., Motoo, Y.	Glycogen synthase kinase 3beta inhibition sensitizes pancreatic cancer cells to Gemcitabine.	J. Gastroenterol.	47	321-333	2012
Okada, H.,	Acyclic retinoid targets platelet-derived growth factor	Cancer Res.	72	4459-4	2012

Honda, M., Campbell, J.S., Sakai, Y., Yamashita, T., Takebuchi, Y., Hada, K., Shirasaki, T., Takabatake, R., Nakamura, M., Sunakozaka, H., ○ Tanaka, T., Fausto, N., Kaneko, S.	signaling in the prevention of hepatic fibrosis and hepatocellular carcinoma development.			471	
○Tanaka, T.	Preclinical cancer chemoprevention studies using animal model of inflammation-associated colorectal carcinogenesis.	Cancers	4	673-700	2012
Nakajima, H., Koizumi, K., ○ Tanaka, T., Ishigaki, Y., Yoshitake, Y., Yonekura, H., Sakuma, T., Fukushima, T., Umehara, H., Ueno, S., Minamoto, T., Motoo, Y.	Loss of HITS (FAM107B) expression in cancers of multiple organs: tissue microarray analysis.	Int. J. Oncol.	41	1347-1357	2012
Yoshimi, K., Hashimoto, T., Niwa, Y., Hata, K., Serikawa, T., ○ Tanaka, T., Kuramoto, T.	Use of a chemically induced-colon carcinogenesis-prone *Apc*-mutant rat in a chemotherapeutic bioassay,	BMC Cancer	12	448	2012
Terakura, D., Shimizu, M., Iwasa, J., Baba, A., Kochi, T., Ohno, T., Kubota, M., Shirakami, Y., Shiraki, M., Takai, K., Tsurumi, H., ○ Tanaka, T., Moriwaki, H.	Preventive effects of branched-chain amino acid supplementation on the spontaneous development of hepatic preneoplastic lesions in C57BL/KsJ-db/db obese mice.	Carcinogenesis	33	2499-2506	2012

Kawabata, K., Tung, N.H., Shoyama, Y., Sugie, S., Mori, T., ○Tanaka, T.	Dietary crocin inhibits colitis and colitis-associated colorectal carcinogenesis in male ICR mice.	Evid. Based Complement. Alternat. Med. (eCAM)	Volume 2012	Article ID 820415	2012
Sakamoto, H., Takenaka, M., Ushimaru, K., ○Tanaka, T.	Use of liquid-based cytology (LBC) and cell blocks from cell remnants for cytologic, immunohistochemical, and immunocytochemical diagnosis of malignancy.	Open J. Pathol.	2	58-65	2012
○Tanaka, T.	Introduction for inflammation and cancer.	Semin. Immunopathol.	35	121-122	2013
Shimizu, M., ○Tanaka, T., Moriwaki, H.	Obesity and hepatocellular carcinoma: targeting obesity-related inflammation for chemoprevention of liver carcinogenesis.	Semin. Immunopathol.	35	191-202	2013
Tanaka, T., Ishikawa, H.	Mast cells and inflammation-associated colorectal carcinogenesis.	Semin. Immunopathol.	35	245-254	2013
Kuno, T., Hatano, Y., Tomita, H., Hara, A., Hirose, Y., Hirata, A., Mori, H., Terasaki, M., Masuda, S., ○Tanaka, T.	Organo-Magnesium Suppresses Inflammation-Associated Colon Carcinogenesis in Male Crj: CD-1 Mice.	Carcinogenesis	34	361-369	2013
Jiang, J., Cao, D., Tsukamoto, T., Wang, G., Jia, Z., Suo, J., Cao, X.	Anticancer effects of 4-vinyl-2,6-dimethoxyphenol (canolol) against SGC-7901 human gastric carcinoma cells.	Oncol. Lett.	5	1562-1566	2013
Tsukamoto, T., Toyoda, T., Mizoshita, T., Tatematsu, M.	Helicobacter pylori infection and gastric carcinogenesis in rodent models.	Semin. Immunopathol.	35	177-190	2013
○ Kimura T, Okamoto K, Miyamoto H, Kimura M, Kitamura S, Takenaka H, Muguruma N, Okahisa T, Aoyagi E, Kajimoto M,	Clinical benefit of high-sensitivity KRAS mutation testing in metastatic colorectal cancer treated with anti-EGFR antibody therapy.	Oncology	82	298-304	2012

Tsuji Y, Kogawa T, Tsuji A, Takayama T.					
Ikematsu, H., Saito, Y., Tanaka, S., Uraoka, T., Sano, Y., Horimatsu, T., Matsuda, T., Oka, S., Higashi, R., ○ Ishikawa, H., Kaneko, K.	The impact of narrow band imaging for colon polyp detection : a multicenter randomized controlled trial by tandem colonoscopy.	J. Gastroenterology	47	1099-1107	2012
Yao, K., Iwashita, A., Nambu, M., Tanabe, H., Nagahama, T., Maki, S., ○Ishikawa, H., Matsui, T., Enjoji, M.	Nature of white opaque substance in the gastric adenoma and cancer as visualized by magnifying endoscopy with narrow-band imaging.	Dig. Endosc.	24	419-425	2012
Nemoto, H., Kataoka, K., ○ Ishikawa, H., Ikata, K., Arimochi, H., Iwasaki, T., Ohnishi, Y., Kuwahara, T., Yasutomo, K.	Reduced diversity and imbalance of fecal microbiota in patients with ulcerative colitis compared to ealthy adult.	Dig. Dis. Sci.	57	2955-2964	2012
Muroi, A., Kiyotani, K., Fujieda, M., ○ Ishikawa, H., Takeshita, T., Iwano, S., Yamazaki, H., Kamataki, T.	Effect of Genetic Polymorphism of CYP2A6 on Individual Susceptibility to Colorectal Tumors in Japanese Smokers.	J. Cancer Therapy	3	207-215	2012
Tanaka, T.,	Mast cell and	Semin.	35	245-25	2012

○Ishikawa, H.	inflammation-associated colorectal carcinogenesis.	Immunopathol.		4	
○ Ishikawa, H., Wakabayashi, K., Suzuki, S., Mutoh, M., Hirata, K., Nakamura, T., Takeyama, I., Kawano, A., Gondo, N., Abe, T., Tokudome, S., Goto, C., Matsuura, N., Sakai, T.	Preventive effects of low-dose aspirin on colorectal adenoma growth in patients with familial adenomatous polyposis : double-blind, randomized clinical trial.	Cancer Medicine	In-press		2012
○ Ishikawa, H., Goto, M., Matuura, N., Murakami, Y., Goto, C., Sakai, T., Kanazawa, K.	A Pilot, Randomized, Placebo-Controlled, Double-Blind Phase 0／Biomarker Study on Effect of Artepillin C-Rich Extract of Brazilian Propolis in Frequent Colorectal Adenoma Polyp Patients.	J. Am. Coll. Nutr.	31	327-337	2012
Nakajima, T., Saito, Y., Tanaka, S., Iishi, H., Kudo, S., Ikematsu, H., Igarashi, M., Saitoh, Y., Inoue, Y., Kobayashi, K., Hisashi, T., Tsuruta, O., Sano, Y., Yamano, H., Shimizu, S., Yahagi, N., Watanabe, T., Nakamura, H.,	Current status of endoscopic resection strategy for large, early colorectal neoplasia in Japan.	Surgical endoscopy	In-press		2013

Fujii, T., Matsuda, T., ○ Ishikawa, H., Sugihara, K.					
Sasazuki S, Inoue M, Iwasaki M, Sawada N, Shimazu T, Yamaji T, Tsugane S; JPHC Study Group.	Combined impact of five lifestyle factors and subsequent risk of cancer: the Japan Public Health Center Study.	Prev. Med.	54	112-6	2012
Kato M, Wei M, Yamano S, Kakehashi A, Tamada S, Nakatani T, Wanibuchi H.	DDX39 acts as a suppressor of invasion for bladder cancer.	Cancer Sci.	103	1363-1369	2012
Wei M, Kakehashi A, Yamano S, Tamano S, Shirai T, Wanibuchi H, Fukushima S.	Lack of Hepatocarcinogenicity of Combinations of Low Doses of 2-amino-3, 8-dimethylimidazo[4,5- f]quinoxaline and Diethylnitrosamine in Rats: Indication for the Existence of a Threshold for Genotoxic Carcinogens.	J. Toxicol. Pathol.	25	209-214	2012
Xie XL, Wei M, Yunoki T, Kakehashi A, Yamano S, Kato M, Wanibuchi H.	Long-term treatment with l-isoleucine or l-leucine in AIN-93G diet has promoting effects on rat bladder carcinogenesis.	Food Chem. Toxicol.	50	3934-3940	2012
Xie XL, Wei M, Kakehashi A, Yamano S, Okabe K, Tajiri M, Wanibuchi H.	Dammar resin, a non-mutagen, inducts oxidative stress and metabolic enzymes in the liver of gpt delta transgenic mouse which is different from a mutagen, 2-amino-3-methylimidazo[4,5-f] quinoline.	Mutat. Res.	748	29-35	2012
Punvittayagul C,	Effects of pinocembrin on the initiation and promotion stages of rat	Asian Pac. J. Cancer Prev.	13	2257-2261	2012

Pompimon W, Wanibuchi H, Fukushima S, Wongpoomchai R.	hepatocarcinogenesis.				
Chung K, Nishiyama N, Wanibuchi H, Yamano S, Hanada S, Wei M, Suehiro S, Kakehashi A.	AGR2 as a potential biomarker of human lung adenocarcinoma.	Osaka City Med. J.	58	13-24	2012
Hoshi H, Sawada T, Uchida M, Iijima H, Kimura K, Hirakawa K, Wanibuchi H.	MUC5AC protects pancreatic cancer cells from TRAIL-induced death pathways.	Int. J. Oncol.	42	887-893	2013
Toba S, Tamura Y, Kumamoto K, Yamada M, Takao K, Hattori S, Miyakawa T, Kataoka Y, Azuma M, Hayasaka K, Amamoto M, Tominaga K, Wynshaw-Boris A, Wanibuchi H, Oka Y, Sato M, Kato M, Hirotsune S.	Post-natal treatment by a blood-brain-barrier permeable calpain inhibitor, SNJ1945 rescued defective function in lissencephaly.	Sci. Rep.	3	1224	2013
○Ogawa K, Hara T, Shimizu M, Ninomiya S, Nagano J, Sakai H, Hoshi M, Ito H, Tsurumi H,	Suppression of azoxymethane-induced colonic preneoplastic lesions in rats by 1-methyltryptophan, an inhibitor of indoleamine 2,3-dioxygenase.	Cancer Sci.	103	951-958	2012

Saito K, Seishima M, Tanaka T, Moriwaki H.					
○Ogawa K, Hara T, Shimizu M, Nagano J, Ohno T, Hoshi M, Ito H, Tsurumi H, Saito K, Seishima M, Moriwaki H.	(-)-Epigallocatechin gallate inhibits the expression of indoleamine 2,3-dioxygenase in human colorectal cancer cells	Oncol. Lett.	4	546-550	2012
○ Kubota M, Shimizu M, Sakai H, Yasuda Y, Terakura D, Baba A, Ohno T, Tsurumi H, Tanaka T, Moriwaki H.	Preventive effects of curcumin on the development of azoxymethane-induced colonic preneoplastic lesions in male C57BL/KsJ-*db/db* obese mice.	Nutr. Cancer	64	72-79	2012
○Hata K, Kubota M, Shimizu M, Moriwaki H, Kuno T, Tanaka T, Hara A, Hirose Y.	Monosodium glutamate-induced diabetic mice are susceptible to azoxymethane-induced colon tumorigenesis.	Carcinogenesis	33	702-707	2012
○Fujiki H, Imai K, Nakachi K, Shimizu M, Moriwaki H, Suganuma M.	Challenging the effectiveness of green tea in primary and tertiary cancer prevention.	J. Cancer Res. Clin. Oncol.	138	1259-1270	2012
Naiki, T., Asamoto, M., Toyoda-Hokaiwado, N., Naiki-Ito, A., Tozawa, K., Kohri, K., Takahashi, S., Shirai, T.	Organ-specific Gst-pi expression of the metastatic androgen independent prostate cancer cells in nude mice.	Prostate	72	533-541	2012
Takahashi, S., Uemura, H., Seeni, A., Tang, M., Komiya, M., Long, N., Ishiguro, H., Kubota, Y., Shirai, T.	Therapeutic targeting of angiotensin II receptor type 1 to regulate androgen receptor in prostate cancer.	Prostate	72	1559-1572	2012

Long, N., Suzuki, S., Sato, S., Naiki-Ito, A., Sakatani, K., Shirai, T., Takahashi, S.	Purple corn color inhibition of prostate carcinogenesis by targeting cell growth pathways.	Cancer Sci.	104	298-303	2013
Kobayashi, D., Kawai, N., Sato, S., Naiki, T., Yamada, K., Yasui, T., Tozawa, K., Kobayashi, T., Takahashi, S., Kohri, K.	Thermotherapy using magnetic cationic liposomes powerfully suppresses prostate cancer bone metastasis in a novel rat model	Prostate			In press
Tang, D., Kryvenko, O.N., Wang, Y., Trudeau, S., Rundle, A., Takahashi, S., Shirai, T., Rybicki, B.A.	2-Amino-1-methyl-6-phenylimidazo[4,5-b]pyridine (PhIP)-DNA adducts in benign prostate and subsequent risk for prostate cancer	Int. J. Cancer			In press
Nakamura, A., Togashi, Y., Orime, K., Sato, K., Shirakawa, J., Ohsugi, M., Kubota, N., Kadowaki, T., Terauchi, Y.	Control of beta cell function and proliferation in mice stimulated by small-molecule glucokinase activator under various conditions.	Diabetologia	55	1745-1754	2012
Shirakawa, J., Tanami, R., Togashi, Y., Tajima, K., Orime, K., Kubota, N.,	Effects of Liraglutide on β-Cell-Specific Glucokinase-Deficient Neonatal Mice.	Endocrinology	153	3066-3075	2012

Kadowaki, T., Goshima, Y., Terauchi, Y.					
Shibata, S., Tada, Y., Asano, Y., Hau, C. S., Kato, T., Saeki, H., Yamauchi, T., Kubota, N., Kadowaki, T., Sato, S..	Adiponectin Regulates Cutaneous Wound Healing by Promoting Keratinocyte Proliferation and Migration via the ERK Signaling Pathway.	J. Immunol.	189	3231-3241	2012
Nakamura, A., Tajima, K., Zolzaya, K., Sato, K., Inoue, R., Yoneda, M., Fujita, K., Nozaki, Y., Kubota, K. C., Haga, H., Kubota, N., Nagashima, Y., Nakajima, A., Maeda, S., Kadowaki, T., Terauchi, Y.	Protection from non-alcoholic steatohepatitis and liver tumourigenesis in high fat-fed insulin receptor substrate-1-knockout mice despite insulin resistance.	Diabetologia	55	3382-3391	2012
Shojima, N., Hara, K., Fujita, H., Horikoshi, M., Takahashi, N., Takamoto, I.,	Depletion of homeodomain-interacting protein kinase 3 impairs insulin secretion and glucose tolerance in mice.	Diabetologia	55	3318-3330	2012

Ohsugi, M., Aburatani, H., Noda, M., Kubota, N., Yamauchi, T., Ueki, K., Kadowaki, T.					
Nakaya, K., Kubota, N.*, Takamoto, I., Kubota, T., Katsuyama, H., Sato, H., Tokuyama, K., Hashimoto, S., Goto, M., Jomori, T., Ueki, K., Kadowaki, T.* (*co-corresponding authors).	Dipeptidyl peptidase-4 inhibitor anagliptin ameliorates diabetes in mice with haploinsufficiency of glucokinase on a high-fat diet.	Metabolism			in press

PLOS ONE

Mouse Model for ROS1-Rearranged Lung Cancer

Yasuhito Arai[1☯], Yasushi Totoki[1☯], Hiroyuki Takahashi[1], Hiromi Nakamura[1], Natsuko Hama[1], Takashi Kohno[2], Koji Tsuta[3], Akihiko Yoshida[3], Hisao Asamura[4], Michihiro Mutoh[5], Fumie Hosoda[1], Hitoshi Tsuda[3], Tatsuhiro Shibata[1]*

1 Division of Cancer Genomics, National Cancer Center Research Institute, Chuo-ku, Tokyo, Japan, **2** Division of Genome Biology, National Cancer Center Research Institute, Chuo-ku, Tokyo, Japan, **3** Division of Pathology and Clinical Laboratories, National Cancer Center Hospital, Chuo-ku, Tokyo, Japan, **4** Thoracic Surgery Division, National Cancer Center Hospital, Chuo-ku, Tokyo, Japan, **5** Division of Cancer Prevention Research, National Cancer Center Research Institute, Chuo-ku, Tokyo, Japan

Abstract

Genetic rearrangement of the *ROS1* receptor tyrosine kinase was recently identified as a distinct molecular signature for human non-small cell lung cancer (NSCLC). However, direct evidence of lung carcinogenesis induced by *ROS1* fusion genes remains to be verified. The present study shows that *EZR-ROS1* plays an essential role in the oncogenesis of NSCLC harboring the fusion gene. *EZR-ROS1* was identified in four female patients of lung adenocarcinoma. Three of them were never smokers. Interstitial deletion of 6q22–q25 resulted in gene fusion. Expression of the fusion kinase in NIH3T3 cells induced anchorage-independent growth *in vitro*, and subcutaneous tumors in nude mice. This transforming ability was attributable to its kinase activity. The ALK/MET/ROS1 kinase inhibitor, crizotinib, suppressed fusion-induced anchorage-independent growth of NIH3T3 cells. Most importantly, established transgenic mouse lines specifically expressing EZR-ROS1 in lung alveolar epithelial cells developed multiple adenocarcinoma nodules in both lungs at an early age. These data suggest that the *EZR-ROS1* is a pivotal oncogene in human NSCLC, and that this animal model could be valuable for exploring therapeutic agents against *ROS1*-rearranged lung cancer.

Citation: Arai Y, Totoki Y, Takahashi H, Nakamura H, Hama N, et al. (2013) Mouse Model for ROS1-Rearranged Lung Cancer. PLoS ONE 8(2): e56010. doi:10.1371/journal.pone.0056010

Editor: John D. Minna, Univesity of Texas Southwestern Medical Center at Dallas, United States of America

Received October 3, 2012; **Accepted** January 4, 2013; **Published** February 13, 2013

Funding: This study was supported by the Program for Promotion of Fundamental Studies in Health Sciences from the National Institute of Biomedical Innovation, National Cancer Center Research and Development Funds (23-A-7 and 23-B-28), Research Grant of the Princess Takamatsu Cancer Research Fund and Grants-in-Aid from the Ministry of Health, Labour and Welfare for the 3rd-term Comprehensive 10-year Strategy for Cancer Control. National Cancer Center Biobank is supported by the National Cancer Center Research and Development Fund, Japan. The funders had no role in study design, data collection and analysis, decision to publish, or preparation of the manuscript.

Competing Interests: The authors have declared that no competing interests exist.

* E-mail: tashibat@ncc.go.jp

☯ These authors contributed equally to this work.

Introduction

Lung cancer is the leading cause of cancer death around the world [1]. Lung adenocarcinoma (LADC), the most common form of non-small-cell lung cancer (NSCLC), comprises several different genomic subsets defined by unique oncogenic alterations, and a considerable proportion of LADC cases harbor driver alterations in the *EGFR*, *KRAS* and *ALK* genes at the mutually exclusive manner with rare exceptions [2–5]. Understanding the molecular basis of cancer allows us to develop therapeutic agents that target genetic druggable aberrations identified in cancer genomes. Tyrosine kinase inhibitors (TKIs) that target the EGFR and ALK proteins are particularly effective in the treatment of LADC carrying *EGFR* mutations and *ALK* fusions, respectively [2–6]. However, the development of an effective TKI requires experimental validation of the genetic aberrations as actionable and druggable. Transgenic mouse models harboring *EGFR* mutations or *EML4-ALK* gene fusions have successfully demonstrated the oncogenic potential of the alterations and the efficacy of TKI therapy [7,8]. Genetic rearrangement of the *ROS1* was recently identified as a distinct molecular signature for human LADC [9–16]. In the present study, we established a mouse model of *ROS1* fusion, and showed that *EZR-ROS1* as an essential driver oncogene in lung carcinogenesis.

Results

Identification of EZR-ROS1 Fusion Gene in LADC of Never-smokers

Whole transcriptome high-throughput sequencing of tumor specimens is one of the most effective methods for identifying fusion oncogenes [17]. Analysis of five LADC cases of never-smokers without *EGFR/KRAS/ALK* alterations using transcriptome sequencing identified 56 reads overriding the in-frame *EZR-ROS1* gene fusion point connecting *EZR* exon 10 to *ROS1* exon 34 in one tumor. RT-PCR analysis of matched non-cancerous tissues confirmed tumor-specific expression of the fusion transcript (Figure 1A). In addition, transcriptome sequencing clearly demonstrated a specific increase in the expression of the fused 3′ portion of *ROS1* (exons 34 to 43) after the breakpoint, suggesting that the *EZR-ROS1* fusion transcript causes aberrant overexpression of *ROS1* tyrosine kinase domain along with the 5′ portion of *EZR* (Figure 1B). SNP array comparative genomic hybridization (array CGH) data showed that this fusion gene was generated by a large interstitial deletion spanning ~41.5 Mb on chromosome 6q22-q25 (Figure 1C). Genomic PCR and sequencing analysis also revealed the deletion of 41.5 Mb causing somatic fusions of the

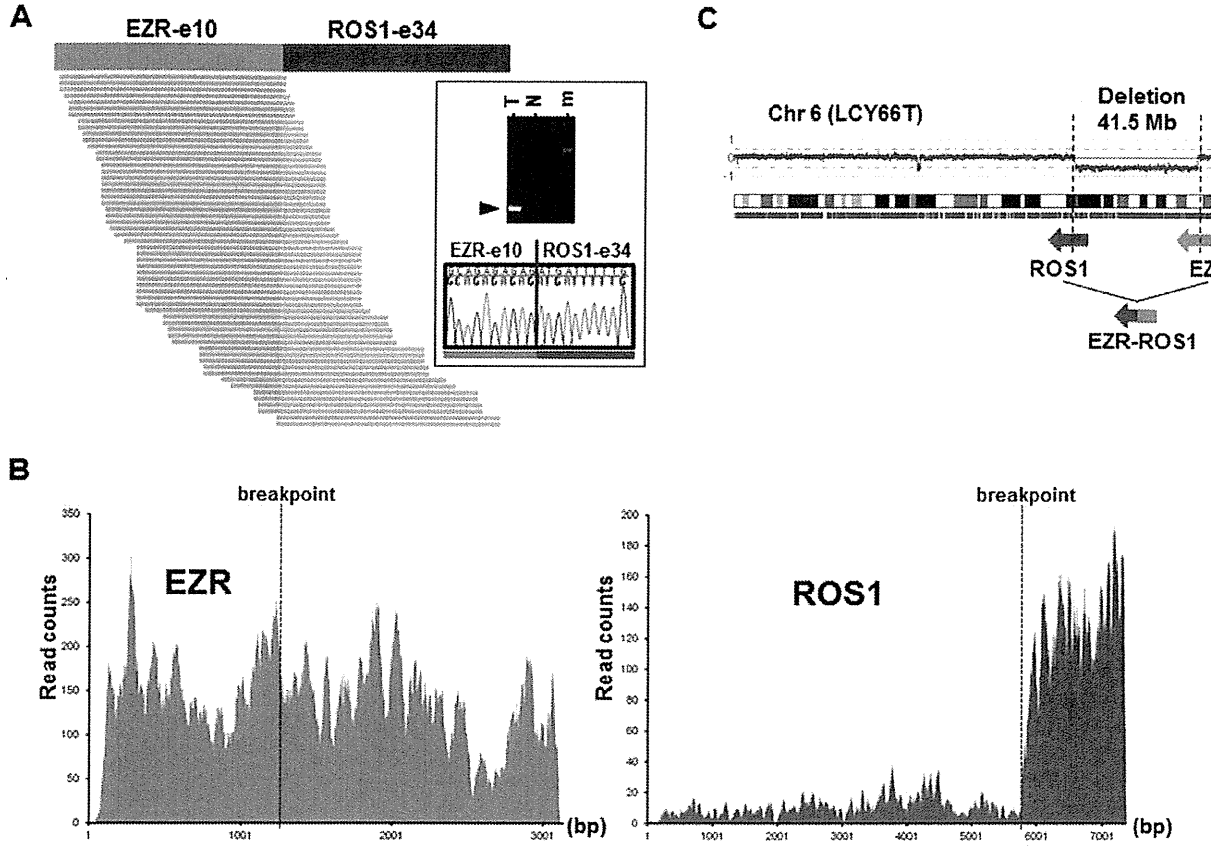

Figure 1. Identification of the *EZR-ROS1* fusion. (A) Junction reads representing *EZR-ROS1* fusion transcripts in LCY66T sample (left). Sanger sequencing of the RT-PCR product validated tumor-specific in-frame fusion transcript (right). m: molecular marker. (B) Expression profiles of *EZR* and *ROS1* in LCY66T. Active expression of the *ROS1* gene was observed after the fusion point. (C) SNP array CGH analysis of the LCY66T. Copy number throughout chromosome 6 is plotted as the log2 ratio.
doi:10.1371/journal.pone.0056010.g001

EZR intron 10 at 6q25 with the *ROS1* intron 33 at 6q22 (Figure S1).

RT-PCR and Sanger sequencing analysis of 569 LADC specimens from Japanese individuals, including the above-mentioned cases (343 cases with early pathological stage and 226 cases with advanced stage), identified four cases harboring this fusion transcript (Figure S2). All four *EZR-ROS1* fusion-positive cases were female, and harbored neither *EGFR/KRAS/HER2* mutations nor *EML4-ALK/KIF5B-RET* fusions. Three cases were poorly differentiated adenocarcinomas of never smokers, and the other was a moderately differentiated adenocarcinoma of a smoker.

Transforming Activity of EZR-ROS1

EZR-ROS1 cDNA isolated from the tumor specimen encoded a protein of 858 amino acids (Figure 2A; GenBank/DDBJ accession number AB698667). The protein connects the FERM domain [18] of ezrin (EZR) with the transmembrane and kinase domains of ROS1, but lacks most of the coiled-coil domain of EZR.

To examine the oncogenic activity of the *EZR-ROS1* fusion *in vitro*, we established stable NIH3T3 clones expressing wild-type EZR-ROS1 and kinase-dead mutant EZR-ROS1 (KD), in which the ATP-binding lysine residue was mutated to methionine (K491M), as well as mutants with serially deleted amino-terminal FERM domains (DL1, DL2 and DL3; Figure 2A). Autophosphorylation of specific tyrosine residues is a crucial event in the activation of distinct signal transduction pathways, and Tyr-2274 of ROS1 is a specific autophosphorylation site essential to induce kinase activity for transformation [19]. In transformation assays, phosphorylation of the Tyr-2274 (corresponding to Tyr-785 in wild type EZR-ROS1 fusion) was observed in a wild-type EZR-ROS1-expressing clone, but was not detected in kinase-dead (KD) and deleted (DL) mutants; this implies that the amino-terminal portion of FERM (1–88 amino acids) is necessary for ROS1 kinase activation (Figure 2B). Wild-type *EZR-ROS1* but not KD/DL mutants specifically induced activation of STAT3 for downstream signaling, and produced significantly anchorage-independent growth (Figure 2C, D). The anchorage-independent growth induced by *EZR-ROS1* was suppressed by treatment with crizotinib, a TKI against ALK/MET/ROS1, whereas the growth induced by another oncogene of lung, *CCDC6-RET* [11] was not (Figure 2E). On the contrary, vandetanib, a TKI against RET/EGFR/VEGFR was effective in inhibiting the colony formation of CCDC6-RET expressing cells, but not in the EZR-ROS1 expressing cells. As shown in Figure 2C, crizotinib treatment suppressed phosphorylation of EZR-ROS1, and inhibit the activation of STAT3.

Next, the NIH3T3 cells were subcutaneously injected into immune-compromised mice. Wild-type EZR-ROS1-expressing clones invariably produced tumors (6/6), while none of the KD

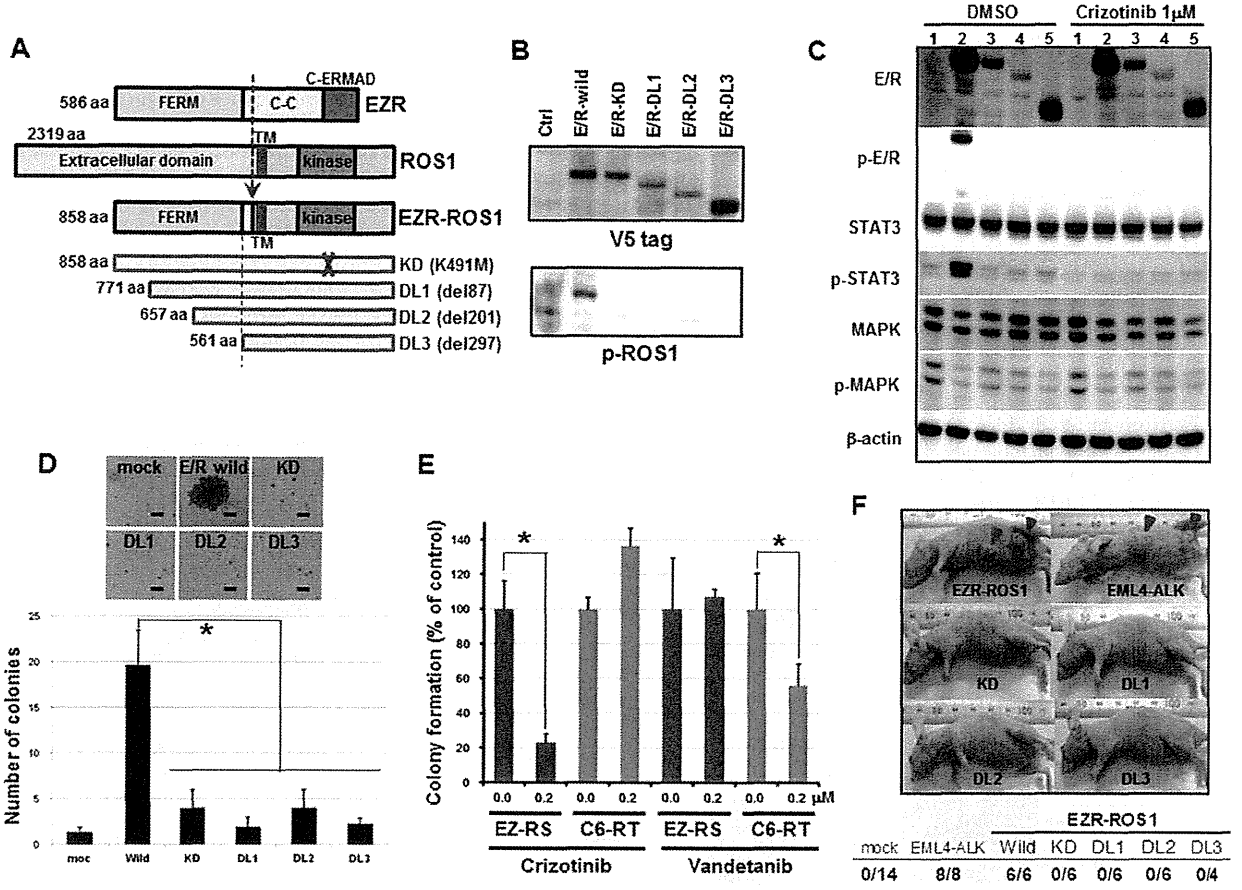

Figure 2. Oncogenic activity of the *EZR-ROS1* fusion gene. (A) Schematic representation of EZR, ROS1, EZR-ROS1, and deletions/mutations of EZR-ROS1 genes. The domain organization is shown. C-C: coiled-coil domain; TM: transmembrane; C-ERMAD: C-terminal ERM associated domain. (B) ROS1 phosphorylation in wild-type and mutant EZR-ROS1 (E/R)-expressing NIH3T3 clones. Cell lysates from each clone were immunoblotted with anti-V5-tag (top) and anti-phosphorylated ROS1 (Tyr-2274, bottom) antibodies. (C) Suppression of ROS 1 kinase activity of EZR-ROS1 by crizotinib inhibits STAT3 activation. NIH3T3 cells transfected with 1: empty vector, 2: wild-type EZR-ROS1, 3: KD 4: DL1, 5: DL3 were serum starved and treated for 2 hr with DMSO or 1 μM of crizotinib, and immunoblotted with the relevant antibodies. β-actin was used as a loading control. E/R: EZR-ROS1, p-E/R: phosphorylated EZR-ROS1 detected with an anti-phosphotyrosine-2274 antibody of ROS1. (D) Soft agar colony formation of wild-type and mutant EZR-ROS1 expressing NIH3T3 clones. A representative picture of colony formation for each clone is plotted at the top (scale bar, 100 μm). The number of colonies obtained for each clone is plotted at the bottom. *P<0.05. (E) Crizotinib-induced suppression of anchorage-independent growth of NIH3T3 cells expressing EZR-ROS1. Bar graph showing the percentage of NIH3T3 colonies induced by *EZR-ROS1* or *CCDC6-RET* after treatment with 200 nM of crizotinib or vandetanib with respect to those formed by DMSO-treated cells. EZ-ROS: EZR-ROS1, C6-RET: CCDC6-RET. *P<0.05. (F) Representative pictures of mice subcutaneously transplanted with NIH3T3 cells expressing wild-type, kinase domain-mutated, or amino-terminal-deleted EZR-ROS1. An EML4-ALK-expressing NIH3T3 clone was used as a positive control. The number of tumors per injection in each transfectant is shown below the photographs.
doi:10.1371/journal.pone.0056010.g002

and DL mutants-expressing clones produced tumors (Figure 2F), confirming that *in vivo* tumorigenic activity of *EZR-ROS1* requires ROS1 kinase activity.

Development of LADC in EZR-ROS1 Transgenic Mice

To further evaluate the role of *EZR-ROS1* in lung carcinogenesis, we generated transgenic mice expressing the fusion gene under the control of a type 2 alveolar epithelium-specific surfactant C gene promoter [20] (Figure 3A). We obtained four independent lines (TgA, B, C and D) with different copy number of the transgene (Figure S3) and detected lung adenocarcinoma nodules in all lines examined except TgD. Analysis of fusion protein expression level among them revealed no expression in TgD (Figure S4). The birth rate of transgene-positive progenies was low in TgC (Transgene-positive F1 progeny number : total F1 number; 1:3), and we failed to keep up a TgC line, then we mainly analyzed one line (TgA), which harbors approximately four copies of the transgene. RT-PCR and immunoblot analysis verified lung-specific *EZR-ROS1* mRNA and protein expression, and indicated phosphorylation of the EZR-ROS1 fusion protein (Figure 3B). Although endogenous *Ezrin* was ubiquitously expressed in many tissues, endogenous *Ros1*-transcript was detected only in stomach, kidney and lung. Protein expression levels of endogenous ROS1 were very weak compared with the levels of the fusion gene in the transgenic mice (Figure S4). Even at the four-week-old, multiple lesions over 1 mm in diameter were detected in the transgenic mice, and tumors occupied over 40% of sectioned surface of lung (Figure 3C and Figure S5). Computed tomography examination

detected multiple nodules in both lungs, and the mice showed reduced survival (Figure 3D, E). Histological examination of lung tumors in the transgenic mouse lines generally demonstrated adenocarcinomas with papillary/lepidic growth pattern (Figure 3C). These lesions were shown to be invasive adenocarcinomas with moderate mitotic activity as revealed by positive Ki-67 staining (Figure S6A). However, in some cases of TgB lines, we observed accumulation of cytoplasmic mucin in tumor cells (Figure S6B).

Despite the presence of multiple tumors in the lungs of the transgenic mice, we failed to detect distant metastasis at necropsy in TgA, B and C mice. Thus, it is likely that expression of *EZR-ROS1* alone is not sufficient to render the cancer cells metastatic.

Discussion

The present study identified *EZR-ROS1* as a pivotal driver oncogene in lung carcinogenesis. Ezrin is ubiquitously expressed in many tissues. In the *EZR-ROS1* fusion detected by RNA sequencing of LADC cases, 5′ portion of *EZR* causes aberrant overexpression of kinase domain of *ROS1*. No evident effect to the transcript levels of the 3′ portion of *EZR* was observed. This might be ascribable to the excess expression of the wild type *EZR* over the fusion gene. We also revealed that ROS1 kinase activation in this fusion requires the N-terminal FERM domain of EZR. FERM associates with many different proteins including phospholipids, the scaffolding proteins EBP50 and E3KARP, and other membrane-associated proteins that may regulate the dimerization or oligomerization of ezrin [21]. Many fusion kinase proteins, including ALK and RET, display constitutive tyrosine kinase activity attributable to dimerization domains in the amino-terminal fusion partner [6,22]. However, another ROS1 fusion protein, FIG-ROS1, which is found in human glioblastoma, cholangiocarcinoma and lung adenocarcinoma, showed no dimerization properties, instead existing as a monomer in the fusion protein despite retaining the coiled-coil domains and a leucine zipper [19]. Therefore, the molecular mechanisms underlying ROS1 activation by the FERM domain remains unclear.

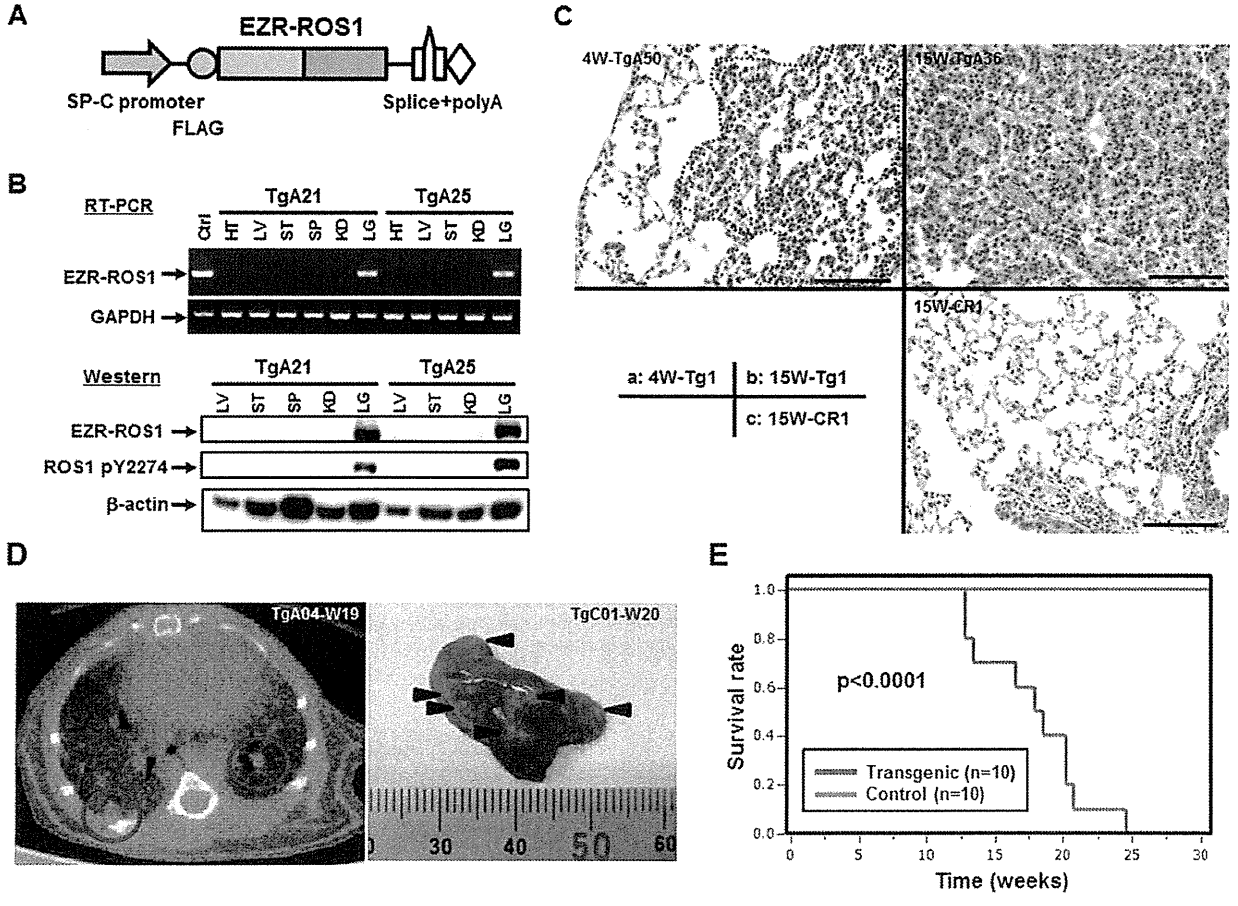

Figure 3. Alveolar epithelium-specific EZR-ROS1 expression generates lung adenocarcinoma *in vivo*. (A) Schematic presentation of the *SP-C/EZR-ROS1/polyA* transgene. (B) Expression of the exogenous *EZR-ROS1* gene in transgenic mice. RT-PCR (top) and immunoblot analysis (bottom) of mouse tissues revealed that EZR-ROS1 was specifically expressed in the lungs of two transgenic mice (TgA21 and TgA25). HT: heart, LV: liver, ST: stomach, SP: spleen, KD: kidney, LG: lung (C) Representative histological analysis of lung lesions in transgenic mice. Hematoxylin-eosin staining shows wide-spread lesions in both 4-week-old and 15-week-old fusion-positive mice. Tg: fusion-positive, CR: fusion-negative. Scale bar, 100 μm. (D) Computed tomography (left) of lungs in TgA04 mouse at week 19. Enhanced lesions in both lungs were detected. Multiple nodular lesions (right) were observed on the pleural surface of the lung in TgC01 mouse at necropsy. (E) Survival curves for transgenic and control mice generated using the Kaplan-Meier method.
doi:10.1371/journal.pone.0056010.g003

The transgenic mice showed an emergence of multiple adenocarcinoma nodules at an early point, and the fast progression of the tumors. These features are broadly similar to the *EML4-ALK* mouse model [8]. Several groups reported that mucinous cribriform pattern and signet ring cell are characteristic histological features of *EML4-ALK* positive human lung cancer [23–25]. Recently, we investigated histopathology of *ROS1*-fusion positive human lung cancers [16]. Although other researchers reported that signet ring cell feature was not common in *ROS1*-rearranged lung cancers [10], we found that 53% of the cases harbored mucinous cribriform or signet ring cell features similar to the *ALK*-rearranged lung cancers but that the rest showed papillary/lepidic growth pattern. *EZR-ROS1*-positive tumors seemed less well differentiated, and showed more frequently histological features of mucinous cribriform or signet ring cell. Our mouse model of *EZR-ROS1* lung cancer generally demonstrated papillary/lepidic growth pattern, but in some cases, we observed accumulation of cytoplasmic mucin in tumor cells, which quite resembles to the characteristic histology reported in *ROS1*-rearranged lung cancer. Currently we have no answer why only part of mice harbored tumors with mucin accumulation.

The *EZR-ROS1* fusion gene was specifically detected in lung cancer specimens of female never-smokers without *EGFR, KRAS,* and *ALK* alterations. It was estimated that ~2% of patients in White and Asian lung cancer cohorts had *ROS1*-rearrangements, which occur at significantly higher rates in younger, non-smoking, female individuals [10,11,16]. Although each alteration is infrequent, *ROS1* fusions with many kinds of 5′ partner genes (*CCDC6, CD74, EZR, FIG, KDELR2, LRIG3, SDC4, SLC34A2 and TPM3*) have been reported in lung, brain, biliary tract, and ovarian cancers [9–16,26–28]. These *ROS1*-rearranged tumors could be targeted therapeutically with specific kinase inhibitors, including crizotinib [10,14,27,29]. Two LADC patients had a remarkable clinical response to crizotinib [10,14]. Thus, our *EZR-ROS1* lung cancer animal model could be valuable for evaluating the therapeutic potential of these compounds and novel drugs as well as biological features of *ROS1*-rearranged lung cancer *in vivo*.

Materials and Methods

Clinical Samples

Tissue specimens from lung cancer patients were provided by the National Cancer Center Biobank, Japan. High-molecular weight genomic DNA and RNA were extracted from fresh frozen tumor specimens and non-cancerous lung tissues. Written informed consent was obtained from each patient. The study protocol was approved by the Ethical Committee of National Cancer Center, Tokyo, Japan.

Analysis of Whole-transcriptome Sequence Data

Insert cDNA libraries (150–200 bp) were prepared from 2 μg of total RNA using the mRNAseq Sample Preparation Kit (Illumina). The libraries were subjected to paired-end sequencing of 50 bp on the HiSeq2000 (Illumina), according to the manufacturer's instructions. Paired-end reads were mapped to known RNA sequences in the RefSeq, Ensembl, and LincRNA databases using the Bowtie program as described previously [30].

RT-PCR, Genomic PCR and Sequencing

Total RNA was reverse-transcribed to cDNA using Superscript III (Life Technologies). cDNA or genomic DNA was subjected to PCR amplification using Ex-Taq (Takara Bio) and primers EZR-e10-CF1 (GAAAAGGAGAGAAACCGTGGAG) and ROS1-e34-CR1 (TCAGTGGGATTGTAACAACCAG). The PCR products were directly sequenced by Sanger sequencing using the BigDye terminator kit (Life Technologies).

SNP Array CGH Analysis

Chromosomal copy number for the tumors was determined using high-resolution SNP arrays (GeneChip Mapping 250K-Nsp array, Affymetrix). Genomic DNA was labeled and hybridized to the SNP arrays according to the manufacturer's instructions, and copy numbers were calculated from the hybridization signals using the CNAG program [31].

Vector Cloning, and Generation of Deletion and Point Mutants

The coding region of *EZR-ROS1* cDNA was obtained by PCR amplification from LCY66 tumor cDNA using Phusion Taq polymerase (New England Biolabs) and primers EZR-H1F1 (CACCATGCCGAAACCAATCAATGTCCGAGTT) and ROS1-H1R1 (ATCAGACCCATCTCCATATCCACTGTG). *EML4-ALK* cDNA and *CCDC6-RET* cDNA were amplified from an *EML4-ALK*-positive primary lung cancer sample (E13;A20) and from a *CCDC6-RET*-positive primary lung cancer sample (C1;R12), respectively. The PCR products were subcloned into a pcDNA3.1D-V5-His plasmid (Life Technologies). Replacement of lysine with methionine at codon 491 in the *EZR-ROS1* gene was performed using a PrimeSTAR site-directed mutagenesis kit (Takara Bio). N-terminal deletion mutants of the FERM domain of *EZR-ROS1* cDNA were constructed by PCR using the primers EZR-FERM-AF (CACCATGGTGGCTGAGGAGCTCATC-CAGGACATC) and ROS1-H1R1 for DL1, EZR-FERM-BF (CACCATGATCAACTATTTCGAGATAAAAAACAAG) and ROS1-H1R1 for DL2, and EZR-FERM-CF (CACCATGAC-CATCGAGGTGCAGCAGATGAAGGC) and ROS1-H1R1 for DL3. The plasmids were transfected into NIH3T3 cells using Lipofectamine 2000 reagent (Life Technologies), and stable clones were isolated by G418 selection (0.7 mg/ml). For the colony formation assay, cells were embedded and cultured in 0.4% soft agar in triplicate and the number of colonies was counted after 21 days. Quantification of anchorage-independent growth under the condition with or without crizotinib (S1068, Selleck) and vandetanib (S1046, Selleck) after 9 days was performed with CytoSelect-96 kit (Cell Biolabs). The compound solution was added to the top layer of soft agar every 3 days.

Immunoblot Analysis

Whole cell lysates were extracted with CelLytic M reagent (#C2978, Sigma), and subjected to SDS-PAGE followed by blotting onto a PVDF membrane. Detection of Western blots was performed with the WesternBreeze Chemiluminescent Immunodetection kit (Life Technologies) using primary antibodies against ROS1 (#9202, Cell Signaling Technology), phosphorylated-ROS1 (Tyr2274) (#3078, Cell Signaling Technology), STAT3 (#610189, BD), phosphorylated-STAT3 (Tyr705) (#9138, Cell Signaling Technology), p44/42 MAPK (#4695, Cell Signaling Technology), phosphorylated-p44/42 MAPK (Thr202/Tyr204) (#9106, Cell Signaling Technology), Ezrin (#4135, Cell Signaling Technology), p53 (#6243, Santa Cruz), and b-actin (#A5441, Sigma).

Suppression of ROS 1 Kinase Activity of EZR-ROS1 by Crizotinib

Transfected NIH3T3 cells (empty vector, wild-type EZR-ROS1, KD/DL mutants) were serum starved for 2 hr, then

added for 2 h with 1% DMSO or 1 μM crizotinib, then the culture medium were changed with standard 10% FBS medium for 10 min. Whole cell lysates were subjected to immunoblot analysis.

Subcutaneous Transplantation in Immune-compromised Mice

A total of 1×10^6 cells were injected subcutaneously into nude mice (BALB/c-nu/nu, CLEA Japan). Mice were monitored daily for tumor formation. All animal procedures were performed with the approval of the animal ethical committee of the National Cancer Center.

Generation and Examination of *EZR-ROS1* Transgenic Mice

FLAG-tagged *EZR-ROS1* cDNA was subcloned into an *SPC-iNOS* plasmid (provided by Dr. Hagiwara), which included an *SPC* promoter and a polyadenylation signal, by replacing the *iNOS* fragment with the cDNA. The expression cassette with the *SPC* promoter was excised from the construct and injected into pronuclear-stage embryos of C57BL/6J mice (Unitech Japan). The copy number of the transgene was determined by Southern blot analysis of DNA from the tails of animals. Transgenic lines were maintained by backcrossing to C57BL/6 mice. Total RNA was isolated from the organs of transgenic mice and subjected to RT-PCR analysis to detect *EZR-ROS1*, endogenous *Ros1*, endogenous *Ezrin* and *Gapdh* mRNAs. To detect EZR-ROS1 protein, endogenous ROS1 and Ezrin in tissues, lysed homogenates were subjected to immunoblot analysis using anti-ROS1, anti-Ezrin and anti-β-actin antibodies. Examination of lung tumors in live animals was performed with an X-ray CT apparatus (eXplore micro-CT, GE Healthcare). Lung tissues were fixed in 10% formalin and paraffin-embedded. Hematoxylin-Eosin staining and immunohistochemistry for Ki67 was performed as previously described [32].

Supporting Information

Figure S1 Detection of *EZR-ROS1* genomic breakpoint junction. Electropherogram for Sanger sequencing of genomic fragments encompassing the *EZR-ROS1* breakpoint junction of LCY66 tumor. Genomic PCR products amplified by the EZR-e10-CF1 and ROS1-e34-CR1 primers were directly sequenced using the EZR-e10-CF1 primer. Numbers above the electropherogram indicate genomic position in chromosome 6 (human genome build 37.3). A genomic fragment of 35 bp of *EZR* intron 10 was inverted within the intron before the fusion to *ROS1* intron 33.
(PDF)

Figure S2 Detection of fusion gene transcripts in clinical samples by RT-PCR. Representative RT-PCR results showing fusion-positive and fusion-negative cases using primers EZR-e10-CF1 and ROS1-e34-CR1. M:molecular marker, NC: negative control. RT-PCR for wild-type *EZR* transcript (primers EZR-e4-CF1 and EZR-e7-CR1) and for *GAPDH* (primers for GAPDH-F and GAPDH-R) is also shown.
(PDF)

Figure S3 Copy number analysis of the transgene in transgenic mice. Genomic DNA was isolated from the tails of transgenic mice generated from pronuclear-stage C57BL/6J embryos. This gDNA was then subjected to Southern blot analysis with a PCR-amplified SPC promoter fragment of 464 bp, generated using primers SPC-pro-F and SPC-pro-R, as a probe. Control samples on the right were comprised of mouse genomic DNA with the indicated copies of the transgene per diploid genome. The ID numbers of mice positive for the transgene are shown at the top.
(PDF)

Figure S4 Gene expressions in transgenic mice. Expression of the genes indicated at left side was investigated by RT-PCR or immunoblot analysis. In RT-PCR, PCR cycles to amplify target genes were indicated at right side. Ezrin showed ubiquitous endogenous expression, however endogenous Ros1 expression was low. No expression of EZR-ROS1 fusion protein was detected in TgD line mice (*). SW480 was used as a negative control for fusion expression. HT: heart, LV: liver, ST: stomach, SP: spleen, KD: kidney, LG: lung.
(PDF)

Figure S5 Lung tumor development in transgenic mice. Lung tissues of TgA mice were cross-sectioned and histologically characterized. The number and size of lesions were surveyed in fusion-positive mice (Tg) and fusion-negative mice (CR) at 4 weeks and 15 weeks after birth. (a) Tumor lesions were classified along its size in diameter (mm), and counted. (b) Tumor occupancy was calculated from the deduced tumor area.
(PDF)

Figure S6 Histological characterization of lung tumors in transgenic mice. (A) Hematoxylin-eosin staining of a mouse lung showing invasive lung adenocarcinoma surrounding a pulmonary vessel (a1). Higher magnification of the tumor (a2). Positive Ki-67 staining in the tumor (a3). Scale bar, 100 μm. (B) Hematoxylin-eosin staining of a mouse lung showing cytoplasmic mucin in lung adenocarcinoma cells (b1). Higher magnification of the tumor (b2). Scale bar, 200 μm.
(PDF)

Acknowledgments

We thank Dr. K. Hagiwara (Saitama Medical University) for providing the SPC-iNOS plasmid, Drs. Y. Nanya and S. Ogawa (University of Tokyo) for providing the CNAG program, and Ms. N. Okada, H. Shimizu, A. Kokubu, T. Urushidate, S. Ohashi and W. Mukai for their excellent technical assistance.

Author Contributions

Conceived and designed the experiments: YA YT TS. Performed the experiments: YA H. Takahashi MM FH. Analyzed the data: YT YA TK HN NH. Contributed reagents/materials/analysis tools: KT AY HA H. Tsuda. Wrote the paper: YA YT TS.

References

1. Jemal A, Bray F, Center MM, Ferlay J, Ward E, et al. (2011) Global Cancer Statistics. CA Cancer J Clin 61: 69–90.
2. Janku F, Stewart DJ, Kurzrock R (2010) Targeted therapy in non-small-cell lung cancer - is it becoming a reality? Nat Rev Clin Oncol 7: 401–414.
3. Gerber DE, Minna JD (2010) ALK inhibition for non-small cell lung cancer: from discovery to therapy in record time. Cancer Cell 18: 548–551.
4. Lovly CM, Carbone DP (2011) Lung cancer in 2010: One size does not fit all. Nat Rev Clin Oncol 8: 68–70.
5. Sasaki T, Jänne PA (2011) New strategies for treatment of ALK-rearranged non–small cell lung cancers. Clin Cancer Res 17: 7213–7218.
6. Soda M, Choi YL, Enomoto M, Takada S, Yamashita Y, et al. (2007) Identification of the transforming EML4-ALK fusion gene in non-small lung cancer. Nature 448: 561–566.